

## **Electronic Supplementary Information**

### **Ultrathin nanosheets constructed CoMoO<sub>4</sub> porous flower with high activity for electrocatalytic oxygen evolution**

Ming Quan Yu,<sup>a</sup> Li Xue Jiang<sup>a</sup> and Hua Gui Yang<sup>\*a</sup>

<sup>a</sup> Key Laboratory for Ultrafine Materials of Ministry of Education, School of Materials Science and Engineering, East China University of Science and Technology, 130 Meilong Road, Shanghai 200237, China.

Correspondence and requests for materials should be addressed to H.G.Y. (hgyang@ecust.edu.cn).

## I. Experimental Section

**Chemicals.** Cobalt (II) chloride hexahydrate ( $\text{CoCl}_2 \cdot 6\text{H}_2\text{O}$ ), ammonium molybdate tetrahydrate ( $(\text{NH}_4)_6\text{Mo}_7\text{O}_{24} \cdot 4\text{H}_2\text{O}$ ), urea and ethanol were purchased from Shanghai Chemical Reagent Co. Ltd. The iridium oxide ( $\text{IrO}_2$ ) was purchased from Strem Chemicals, Inc. Nafion (5 wt%) was obtained from Sigma-Aldrich. Ultrapure water ( $18.2 \Omega \text{ cm}^{-2}$  resistivity) was used for all aqueous solution. All chemicals were of analytical grade and used as received without further purification.

**Hydrothermal synthesis of  $\text{CoMoO}_4$  sample.** In a typical procedure,  $\text{CoCl}_2 \cdot 6\text{H}_2\text{O}$  (0.5 mmol),  $(\text{NH}_4)_6\text{Mo}_7\text{O}_{24} \cdot 4\text{H}_2\text{O}$  (0.071 mmol) and  $\text{CO}(\text{NH}_2)_2$  (5 mmol) were dissolved in 36 mL of deionized (DI) water and stirred to form a clear solution at room temperature. The as-formed homogenous solution was then transferred into a Teflon-lined stainless steel autoclave, which was sealed, maintained at  $120 \text{ }^\circ\text{C}$  for 12 h, and then allowed to cool to room temperature naturally. Product was collected by centrifugation at 5000 rpm for 5 min, washed with DI water and ethanol and dried at  $60 \text{ }^\circ\text{C}$  for 12 h.

**Synthesis of  $\text{Co}_3\text{O}_4$  sample.** The comparative  $\text{Co}_3\text{O}_4$  sample was prepared by a facile two-step method. After a similar hydrothermal process without adding  $(\text{NH}_4)_6\text{Mo}_7\text{O}_{24} \cdot 4\text{H}_2\text{O}$  described above, the product was calcined in air at  $400 \text{ }^\circ\text{C}$  for 3 h. The resulting powders can be collected after the tube furnace cooling down to room temperature.

**Hydrothermal synthesis of  $\text{Co}(\text{CO}_3)_{0.35}\text{Cl}_{0.20}(\text{OH})_{1.10}$  sample.** The pure  $\text{Co}(\text{CO}_3)_{0.35}\text{Cl}_{0.20}(\text{OH})_{1.10}$  sample was prepared by a similar hydrothermal process without adding  $(\text{NH}_4)_6\text{Mo}_7\text{O}_{24} \cdot 4\text{H}_2\text{O}$  described above. Product was collected by centrifugation at 5000 rpm for 5 min, washed with DI water and ethanol and dried at  $60 \text{ }^\circ\text{C}$  for 12 h.

**Electrochemical measurements.** 4 mg of catalyst powder and 40  $\mu\text{L}$  Nafion solution (5 wt%) were dispersed in 1 mL of 4:1 v/v water/ethanol by at least 30 min sonication to form a homogeneous ink. Then 5  $\mu\text{L}$  of the catalyst ink was loaded onto a glassy carbon electrode of 3 mm in diameter (loading  $0.285 \text{ mg cm}^{-2}$ ). For comparison, the electrodes were also modified with  $\text{IrO}_2$ . Finally, the as-prepared catalyst films were dried at room temperature.

All electrochemical studies were performed using a CHI 660 potentiostat (CH Instruments, China) in a three-electrode setup in 1 M KOH aqueous solution. The reference electrode and counter electrode were Ag/AgCl electrode (3.5 M KCl) and platinum mesh, respectively.

The electrocatalytic activity of the catalysts towards OER was examined by polarization curves using linear sweep voltammetry (LSV) with a sweep rate of 5 mV

s<sup>-1</sup> in 1 M KOH at room temperature. All of the potentials in our manuscript were calibrated to a reversible hydrogen electrode (RHE) by following calculations:  $E_{\text{RHE}} = E_{\text{Ag/AgCl}} + 0.059 \times \text{pH} + 0.205$ . All LSV polarization curves were not corrected. AC impedance measurements were carried out in the same configuration when the working electrode was biased at overpotential of 350 mV from 10<sup>5</sup> Hz to 1 Hz with an AC voltage of 5 mV. Galvanostatic measurement ( $j = 10 \text{ mA/cm}^2$ ) was performed to evaluate the long-term stability.

**Characterizations.** The morphology and structure of the samples were characterized by scanning electron microscopy (SEM, Hitachi S4800) and transmission electron microscopy (TEM, JEM 2100, 200 kV). Brunauer-Emmett-Teller (BET) surface area measurements were performed at 77K on a Micromeritics ASAS 2460 adsorption analyzer in N<sub>2</sub>-adsorption mode. The sample was degassed at 150 °C for 24 h under vacuum prior to the measurements. The crystal structure was determined by X-ray diffraction (XRD, D/max2550V). Further, the chemical states of the elements in catalysts were studied by X-ray photoelectron spectroscopy (XPS, Kratos Axis Ultra DLD), and the binding energy of C 1s peak at 284.8 eV was taken as an internal standard.

## II. Supporting Figures

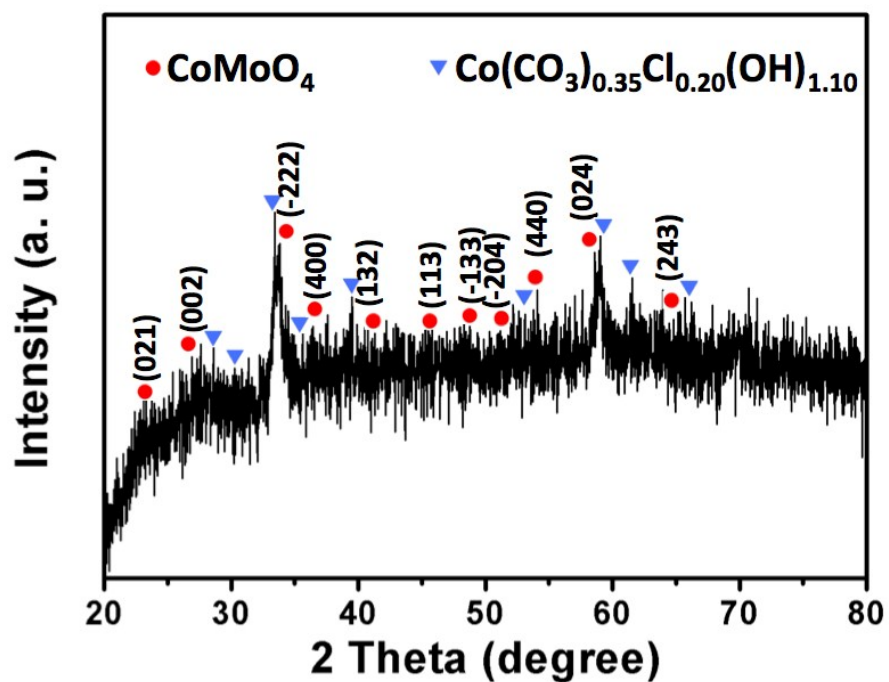


**Figure S1.** XRD pattern of the as-prepared sample. Circle:  $\text{CoMoO}_4$  (JCPDS card No. 21-0868). Triangle:  $\text{Co}(\text{CO}_3)_{0.35}\text{Cl}_{0.20}(\text{OH})_{1.10}$  (JCPDS No. 38-0547).

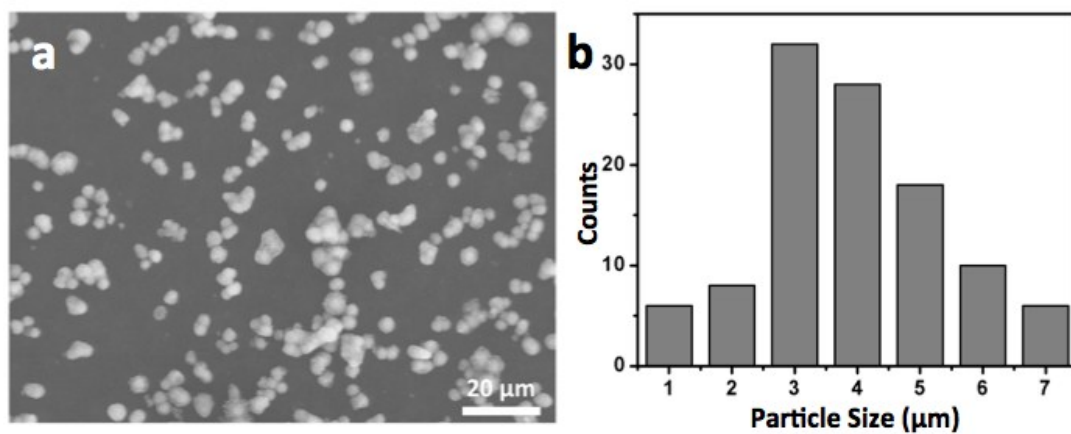


**Figure S2.** (a) SEM image of synthesized  $\text{CoMoO}_4$  micro-flowers. (b) The particle size histogram of synthesized  $\text{CoMoO}_4$  micro-flowers obtained from (a).

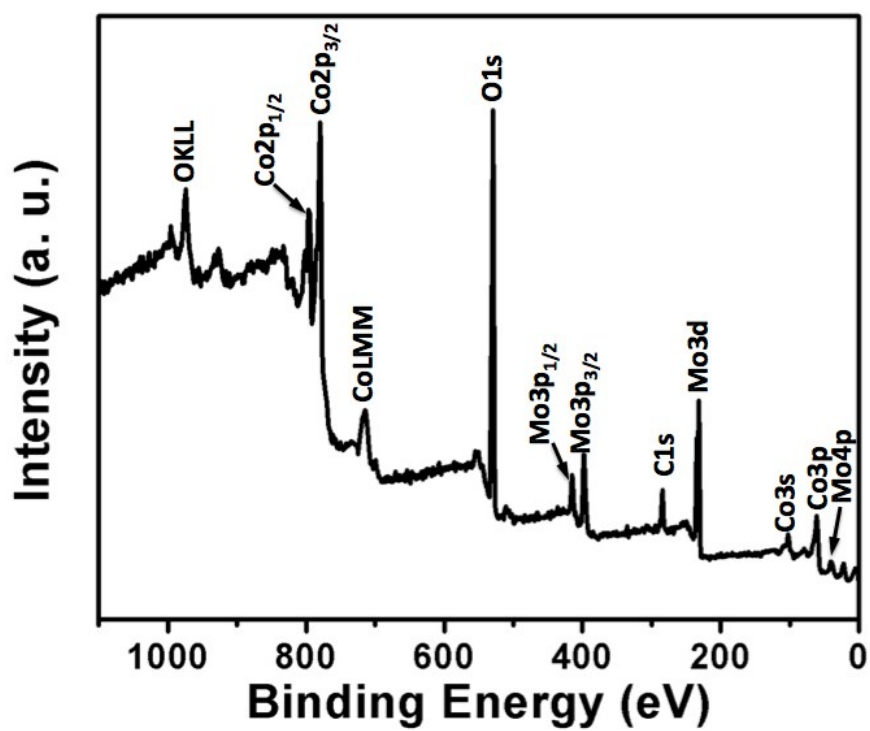
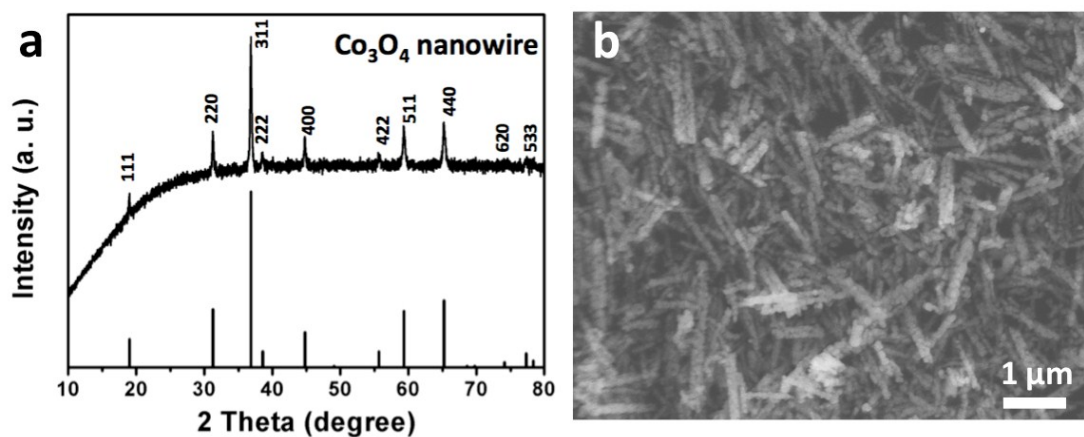
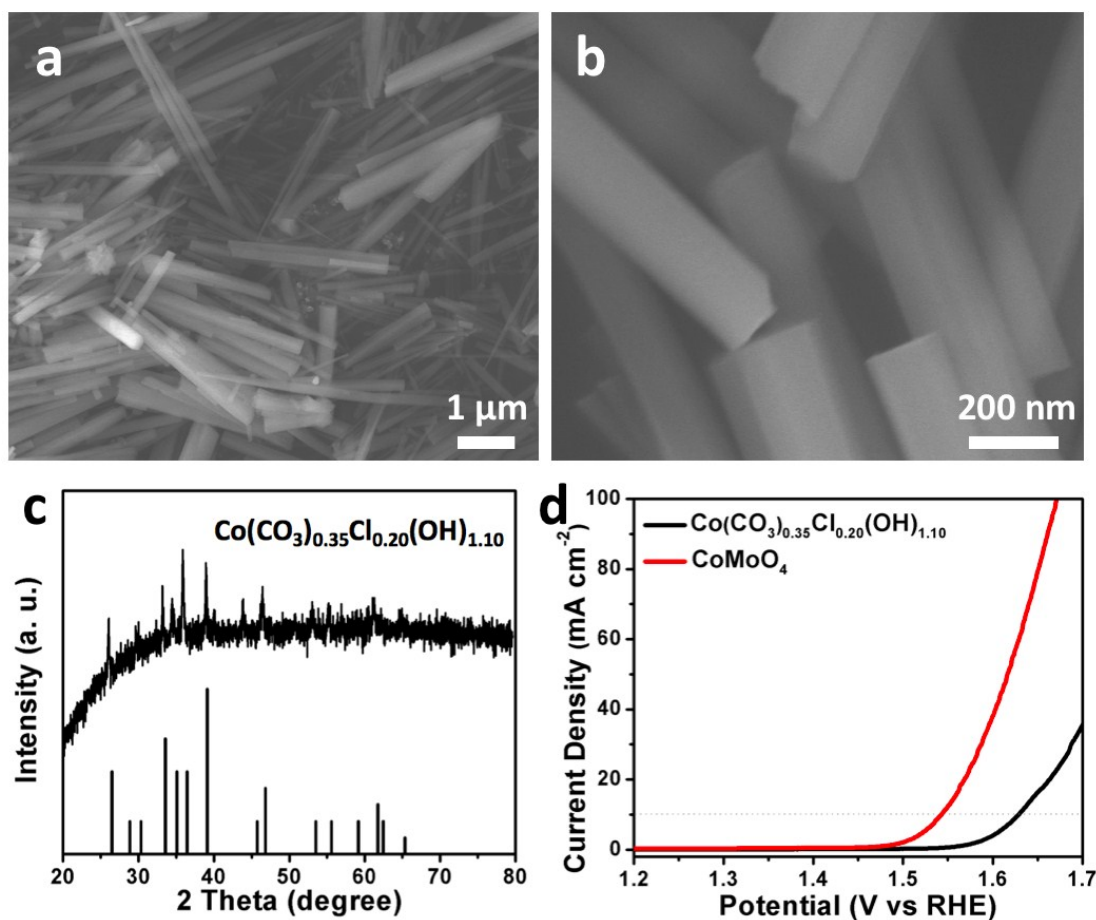


Figure S3. XPS survey spectrum of as-prepared CoMoO<sub>4</sub> sample.



**Figure S4.** (a) XRD pattern of  $\text{Co}_3\text{O}_4$  sample. All the diffraction peaks of the prepared  $\text{Co}_3\text{O}_4$  sample can be indexed to the cubic  $\text{Co}_3\text{O}_4$  (JCPDS No. 43-1003). (b) SEM image of  $\text{Co}_3\text{O}_4$  sample.



**Figure S5.** (a) Low-magnification and (b) high-magnification SEM images of pure  $\text{Co}(\text{CO}_3)_{0.35}\text{Cl}_{0.20}(\text{OH})_{1.10}$  nanowires. (c) XRD pattern of the  $\text{Co}(\text{CO}_3)_{0.35}\text{Cl}_{0.20}(\text{OH})_{1.10}$  nanowires, All the diffraction peaks of the prepared  $\text{Co}(\text{CO}_3)_{0.35}\text{Cl}_{0.20}(\text{OH})_{1.10}$  sample can be indexed to the standard card of  $\text{Co}(\text{CO}_3)_{0.35}\text{Cl}_{0.20}(\text{OH})_{1.10}$  (JCDPS No. 38-0547). (d) Polarization curves for OER on pure  $\text{Co}(\text{CO}_3)_{0.35}\text{Cl}_{0.20}(\text{OH})_{1.10}$  nanowires and  $\text{CoMoO}_4$  micro-flowers, which shows that  $\text{Co}(\text{CO}_3)_{0.35}\text{Cl}_{0.20}(\text{OH})_{1.10}$  nanowires have little OER activity.

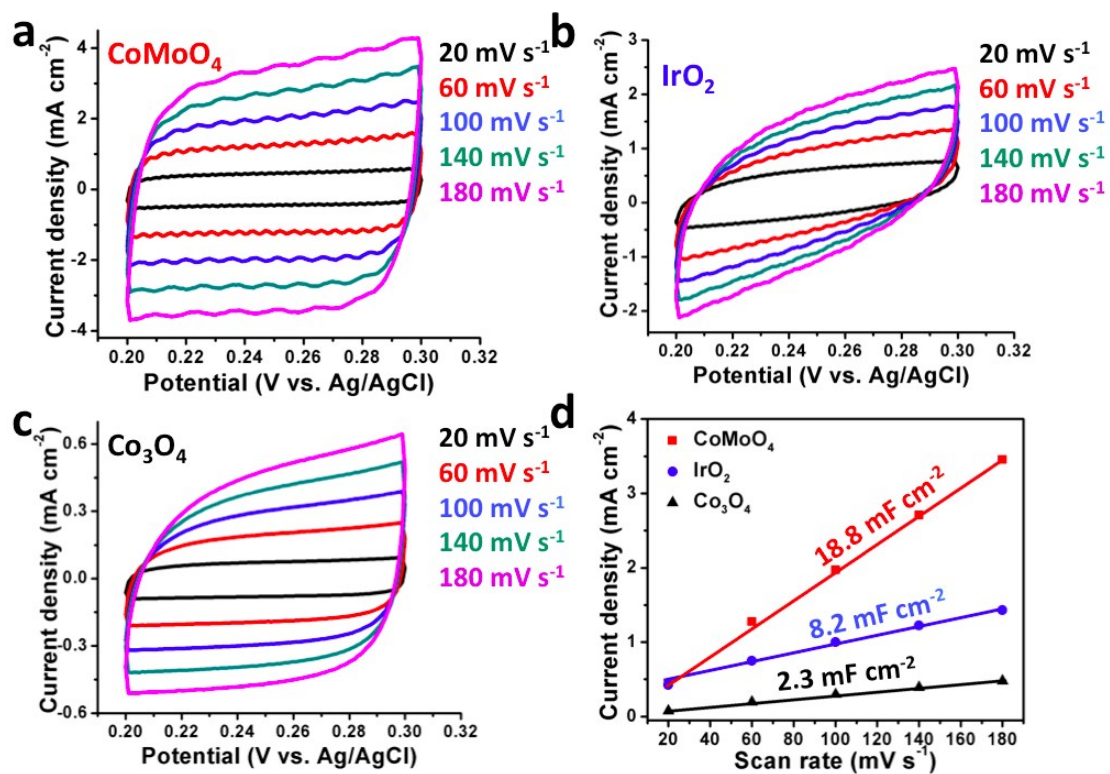


**Figure S6.** (a-c) EDLC curves of CoMoO<sub>4</sub>, IrO<sub>2</sub> and Co<sub>3</sub>O<sub>4</sub> respectively at different scan rates in a potential window where no Faradaic process occur (0.2-0.3 V vs. Ag/AgCl). (d) Plots of current densities at 0.25 V vs scan rates of CoMoO<sub>4</sub>, IrO<sub>2</sub> and Co<sub>3</sub>O<sub>4</sub> respectively.

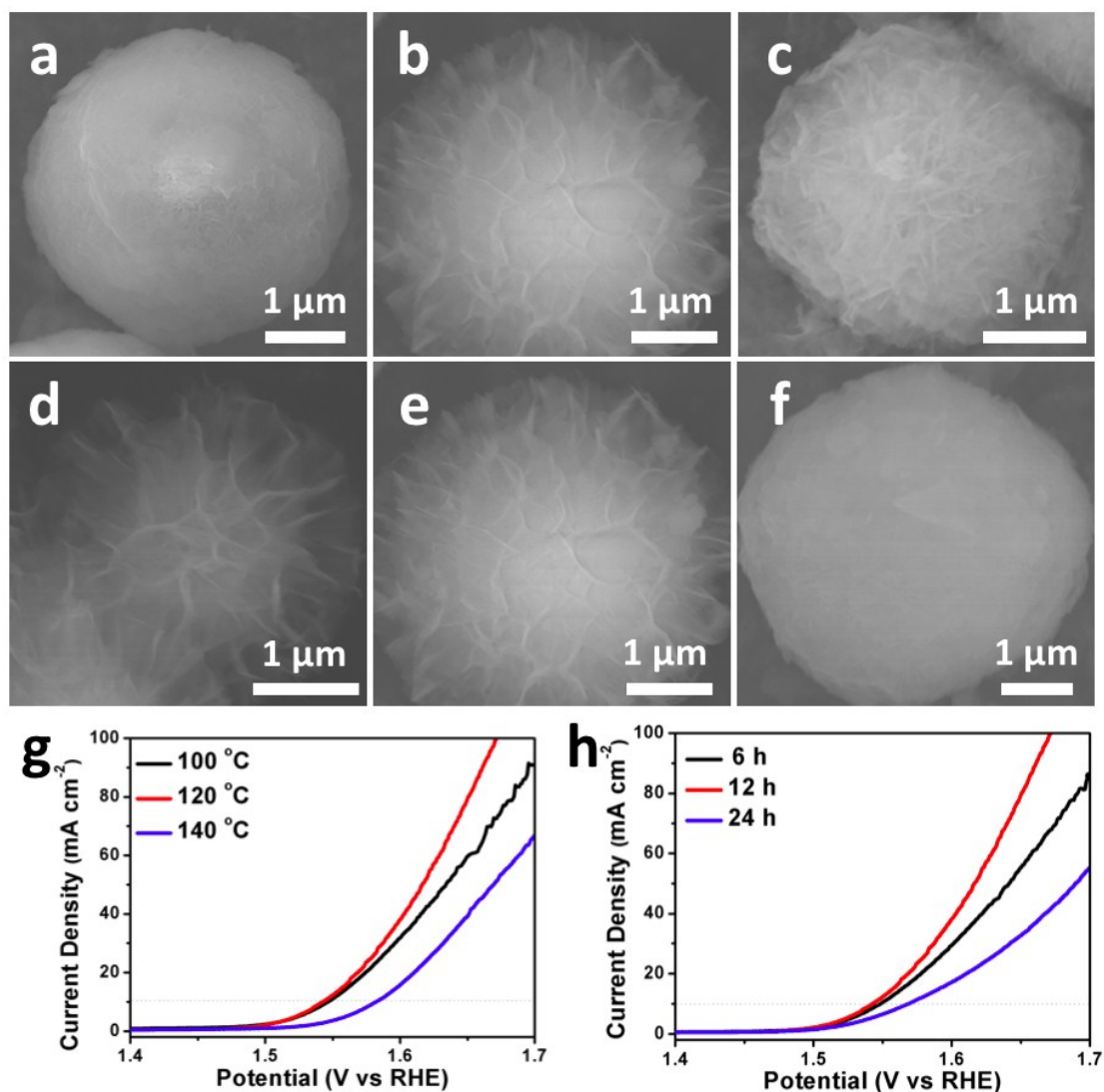


**Figure S7.** SEM images of the CoMoO<sub>4</sub> procedure with different hydrothermal reaction conditions: (a) at 100 °C for 12h, (b) at 120 °C for 12h, (c) at 140 °C for 12h, (d) at 120 °C for 6h, (e) at 120 °C for 12h, (f) at 120 °C for 24h; (g) is the corresponding polarization curves for OER of (a-c); and (h) is the corresponding polarization curves for OER of (d-f).

To study the formation mechanism of the spherical CoMoO<sub>4</sub> architecture, a series of experiments with different reaction conditions were carried out. Under hydrothermal environment at 120 °C, the CoMoO<sub>4</sub> crystallites began to grow along the layered plane and assembled to form sphere-shape structures as the reaction continued, leading to the formation of hierarchical CoMoO<sub>4</sub> micro-flowers. As shown in Fig. S7, the reaction temperature and the reaction time can affect the morphology of the synthesized CoMoO<sub>4</sub> product. Of which, the product obtained at 120 °C for 12 h has the morphology of sphere constructed by ultrathin nanosheets. Moreover, benefitting from the high specific surface area and constituent nanosheet with an ultrathin thickness, it exhibits superior electrocatalytic activity.

**Table. S1. Comparison of the electrocatalytic activity of CoMoO<sub>4</sub> to recently reported Co-based OER electrocatalysts in basic electrolyte<sup>†</sup>**

Catalysts (mg/cm <sup>2</sup> )	Electrolyte	Onset potential (mV)	Overpotential at 10 mA/cm <sup>2</sup> (mV)	Tafel (mV/decade)	Ref.
Co <sub>3</sub> O <sub>4</sub> /N-rmGO/Ni foam (1.0)	1M KOH	/	310	67	<i>Nat. Mater.</i> , 2011, 10, 780-786.
<b>CoMoO<sub>4</sub> (0.285)</b>	<b>1M KOH</b>	<b>235</b>	<b>312</b>	<b>56</b>	<b>this work</b>
CoSe <sub>2</sub> (0.142)	0.1M KOH	/	320	44	<i>J. Am. Chem. Soc.</i> , 2014, 136, 15670-15675.
(Ln <sub>0.5</sub> Ba <sub>0.5</sub> )CoO <sub>3-x</sub> (0.25)	0.1M KOH	/	~330 (Ln=Pr)	/	<i>Nat. Commun.</i> , 2013, 4, 2439.
crumpled graphene-CoO (0.7)	1M KOH	/	340	71	<i>Energy Environ. Sci.</i> , 2014, 7, 609-616.
NiCo <sub>2.7</sub> (OH) <sub>x</sub>	1M KOH	250	350	65	<i>Adv. Energy Mater.</i> , 2015, 5, 1402031.
CoMn-LDH (0.142)	1M KOH	/	350	43	<i>J. Am. Chem. Soc.</i> , 2014, 136, 16481-16484.
CoCo-NS (0.07)	1M KOH	307	353	45	<i>Nat. Commun.</i> , 2014, 5, 4477.
Ba <sub>0.5</sub> Sr <sub>0.5</sub> Co <sub>0.8</sub> Fe <sub>0.2</sub> O <sub>3-x</sub>	0.1M KOH	314	~362	~48	<i>Science</i> , 2011, 134, 1383-1385.
exfoliated NiCo LDH /carbon paper (0.08)	1M KOH	/	367	40	<i>Nano Lett.</i> , 2015, 15, 1421-1427
reduced Co <sub>3</sub> O <sub>4</sub> (0.136)	1M KOH	290	~410	72	<i>Adv. Energy Mater.</i> , 2014, 4, 1400696.
SrNb <sub>0.1</sub> Co <sub>0.7</sub> Fe <sub>0.2</sub> O <sub>3-δ</sub>	0.1M KOH	260	420	90	<i>Angew. Chem. Int. Ed.</i> , 2015, 54, 1-6.
Mn <sub>3</sub> O <sub>4</sub> /CoSe <sub>2</sub> (0.2)	0.1M KOH	/	450	49	<i>J. Am. Chem. Soc.</i> , 2012, 134, 2930-2933.
mesoporous Co <sub>3</sub> O <sub>4</sub>	1M KOH	/	476	/	<i>Nano Res.</i> , 2013, 6, 47-54.
Au/mCo <sub>3</sub> O <sub>4</sub>	0.1M KOH	300	650	46	<i>ChemSusChem</i> , 2014, 7, 82-86.

<sup>†</sup> The table was built by the column of the overpotential that reaches to the current density of 10 mA cm<sup>-2</sup> in a descending order.